Proteomic analysis of opsins and thyroid hormone-induced retinal development using isotope-coded affinity tags (ICAT) and mass spectrometry

W. Ted Allison, Kathy M. Veldhoen, Craig W. Hawryshyn

Department of Biology, University of Victoria, Victoria, British Columbia, Canada

Purpose: Analyses that reveal the relative abundance of proteins are informative in elucidating mechanisms of retinal development and disease progression. However, popular high-throughput proteomic methods do not reliably detect opsin protein abundance, which serve as markers of photoreceptor differentiation. We utilized thyroid-hormone (TH) treatment of rainbow trout (*Oncorhynchus mykiss*) as a model of cone apoptosis and cone regeneration. We used this model to investigate if emerging proteomic technology allows effective analysis of retinal development and opsin protein abundance. We also sought to begin a characterization of proteomic changes in the retina occurring with TH treatment and address whether TH affects proliferation or photoreceptor differentiation.

Methods: Retinal homogenates were prepared from control and TH-treated fish. Peptides from control and treated homogenates were differentially labeled, using isotope-code affinity tags (ICAT) and analyzed using capillary liquid chromatography-electrospray ionization-tandem mass spectrometry (capLC-ESI-MS/MS). This method identifies proteins and quantifies their relative abundance between two samples.

Results: The relative abundance of many retinal proteins changed during TH treatment. These included proteins from every functional class. We detected 1,684 different peptides, and our quantification suggests that 94 increased and 146 decreased in abundance more than 50% during TH treatment. Cell-cycle proteins appear to be increased, consistent with TH-inducing cell proliferation, similar to its effect in *Xenopus*. Other proteins associated with retinal development, such as ΔA and tubulins, changed in abundance during TH treatment. Rod opsin and three cone opsins were identified and the relative abundance of each changed with TH treatment.

Conclusions: ICAT and capLC-ESI-MS/MS are an effective complement to other molecular approaches that investigate the mechanisms of retinal development. Unlike other proteomic techniques, this approach does not require development of species- or tissue-specific methodology, such as characterizing two dimensional (2D) gels or antibodies, in order to be practical as a high-throughput approach. Importantly, this technology was able to assess the relative abundance of opsin proteins. These findings represent the first high-throughput proteomic analysis of the retina and demonstrate the technique's ability to provide useful information in retinal development.

The characterization of retinal proteins is valuable in understanding mechanisms of retinal development, disease and repair. Such studies can be effective complements or alternatives to high-throughput analyses of the transcriptome such as those accomplished by microarrays and serial analysis of gene expression [1-3]. For example, proteomic analyses may be favoured over transcriptome analyses when mRNA abundance does not reflect protein abundance [4]. Furthermore, transcriptome analysis is unable to assess post-translational modifications that can alter protein function.

To date, characterization of the retinal proteome has been accomplished using two dimensional (2D) gels or panels of antibodies. Recent efforts on several animal models have focused on measures that will allow these strategies to become high-throughput. One approach has been to catalog the identities of protein spots on 2-D gels. This approach has established the prerequisite background to allow characterization of porcine, bovine, and murine retinal proteomes [1,5-8]. Other efforts have focussed on characterizing panels of relevant antibodies for their utility in zebrafish immunohistochemistry [9]; at least for some targets, this approach can be quantitative [10].

We utilized *Oncorhynchus mykiss*, a salmonid fish, as a model of cone death and cone regeneration. During natural development, ultraviolet-sensitive (UVS) cones, which are homologs of mammalian "s-cones" or "blue cones," die from the retina of salmonids by apoptosis [11-14]. In *Oncorhynchus mykiss*, this UVS cone death appears to be associated with smoltification, a metamorphic transition that prepares migratory populations for physiological requirements of the marine environment. Thyroid hormone (TH) peaks during smoltification, and treatment of salmonids with TH can mimic many aspects of smoltification [15,16], including changes in the visual system such as UVS cone death [12,14,17-19]. Of notable significance, UVS cones reappear into the retina later

Correspondence to: Dr. Craig W. Hawryshyn, Department of Biology, Queen's University, Kingston, Ontario, Canada, K7L 3N6; Phone: (613) 533-6000 x78529; FAX: (613) 533-6617; email: craig.hawryshyn@queensu.ca.

Dr. Allison is now at the Department of Molecular, Cellular & Developmental Biology, Ann Arbor, MI.

in the salmonid life history, possibly during sexual maturation and the return migration to freshwater spawning grounds [12,14,18,20-22]. The quickly growing trout retina has proliferating cells in the established retina [23] that respond to injury [12,24,25] and support the regeneration of the UVS cone [12,14].

Both UVS cone death and regeneration can be induced by manipulations of TH [12,14,17-20,26]. This provides a controlled onset time for developmental events of interest. TH treatment is known to produce several other effects in the retina, including changes in rhodopsin/porphyropsin levels [27-30], cell size/density [20], proliferation [12,14,31,32], and changes in deiodinase levels [33]. Deiodinases are enzymes that activate and deactivate circulating TH in an organ-specific manner. The retina of teleosts, *Xenopus*, and mammals express deiodinases [3,32-35] as measured by enzyme activity and in situ hybridization. Salmonid fishes, including rainbow trout, have surprisingly high levels of deiodinase activity [33], indicating that TH metabolism has a substantive role in salmonid retinal physiology and acts primarily at the level of retinal cells to effect initiate their development.

Analyses of retinal development in salmonids have mostly been limited to histology [11,17,18,20,21,36-46], electrophysiology [13,14,19,37,45,47-50], and transcriptome analyses [13,51]. We have recently worked with existing antibodies [12,14,25,52] and developed novel antibodies [12,14,53] to examine proteins in trout retinal development. Few other antibodies have been characterized in salmonid retina [54-65]. We sought a proteomic approach to investigate the unique developmental events in rainbow trout retina during TH treatment. Whereas several papers have been successful using 2D gels on other trout tissues [66-68], we noted that strategies using antibodies or 2D gels require substantial investment in preparatory experiments before high-throughput analyses can be fruitful. Antibodies do not allow discovery of novel gene products, a particular interest of ours in exploring our model of how stem cells regenerate cones [14]. Further, we noted that the detection limits of 2-D gels prohibit reliable detection of opsin proteins. Indeed, several thorough analyses of retina using 2-D gels have failed to identify rod or cone opsins, despite rod opsin being one of the most abundant retinal proteins [1,5-8]. The ability to identify opsin abundance has often been used as an effective marker for rod and cone differentiation, and as a proxy for disease progression.

We have investigated an evolving proteomic technique that utilizes isotope-coded affinity tags (ICAT) and mass spectrometry (MS) to simultaneously quantify and identify peptides. The method reports relative abundances of peptides from two protein pools [69]. All cysteine-containing proteins are labeled with a biotin-based tag (Figure 1). The tag has either a heavy or light isotope, owing to the presence of nine deuterium atoms in the heavy isotope, and thus the peptides from each pool differ in mass by 9 Da (Figure 1, Figure 2). The protein pools are combined and then trypsinized. Trypsin-derived peptides are examined in a tandem MS. Pairs of peptides from each protein pool are then recognized by their 9 Da mass differential, and their relative abundance can be quantified. The associated proteins are finally identified using collision-induced decomposition fragments of the selected peptides in interrogation of peptide fragment databases. The technique has only recently been applied to tissues as morphologically complex as the retina. Although this technique is known to be a quantitative methodology, with examples of this in the literature [69-74], our aim was to evaluate the methodology, look for differences, and present them for reference and as guideposts for future research. This research represents a starting point in the literature for future research.

We find that despite the relatively limited genetic databases currently available for our model organism, the technique revealed several peptides from proteins of unknown function and demonstrated that many proteins changed in abundance during TH treatment. Furthermore, the technique identified changes in the relative abundance of rod opsin and three cone opsin proteins.
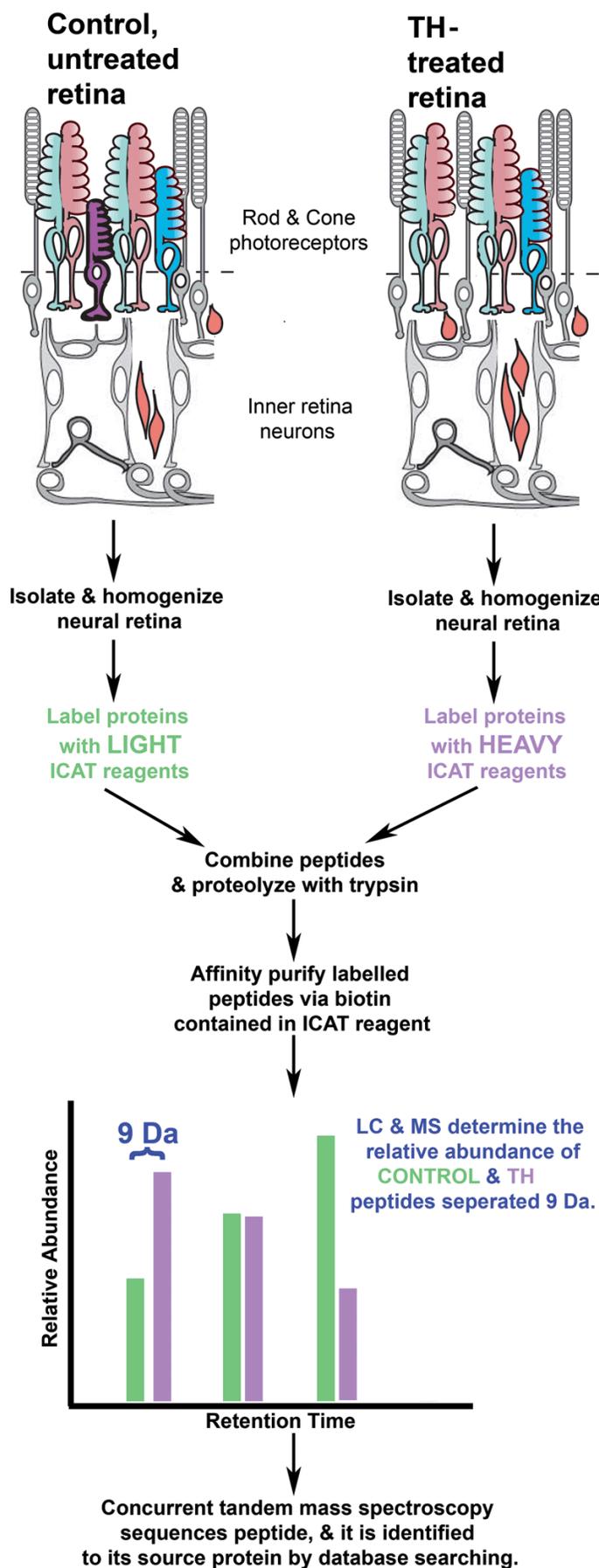
METHODS

Animals and sample preparation: Rainbow trout were obtained from the Vancouver Island Trout Hatchery, Duncan, British Columbia, Canada. Fish were housed at the University of Victoria Aquatics Facility and maintained at 15±1 °C. A 12 h light:12 h dark photoperiod was provided by fluorescent lights (Stanpro FU32T8/65K/8 6500K, Saint-Laurent, QC). Fish were maintained in these conditions for at least four weeks prior to sampling. Fish were fed three times per week with Moore-Clark Trout AB feed. Care of the fish and all procedures were in accordance with and approved by the University of Victoria Animal Care Committee under the auspices of the Canadian Council for Animal Care.

Rainbow trout parr were treated for nine days in an exogenous bath of L-thyroxine sodium salt (Sigma, St. Louis, MO) dissolved in 0.1 N NaOH to a final concentration of 300 µg/l. Water was changed daily. Control fish were treated identically, but only vehicle (NaOH without L-thyroxine) was added to their water. Control and TH-treated fish had average standard lengths (±1 standard deviation [SD]) of 79±9 and 82±9 mm (n=5), respectively.

Starting 4 h after initiation of the light cycle, trout were dark-adapted for 1 h, sacrificed by MS-222 overdose followed by cervical transection, and the neural retina was dissected in ice-cold PBS. Following dissection, the entire retinas were immediately placed in 500 µl of ice-cold buffer (30 mM Tris-HCl pH 7.5, 10 mM EGTA, 5 mM EDTA, 250 mM sucrose, 1% octylglucopyranoside [Sigma]). Each retina was then homogenized on ice, using a disposable Kontes Pellet Pestle with cordless motor tissue grinder (Kimble Kontes, Vineland, NJ) for approximately 1 min, vortexed for 15 s, and microcentrifuged at 4 °C at 10,000x g for 10 min. The resulting supernatant was collected and used for ICAT labeling.

Production and analysis of ICAT-labeled peptides: Production and analysis of ICAT-labeled peptides was performed by the University of Victoria Genome British Columbia Proteomics Center. All procedures were performed according

Figure 1. Methodology for identifying peptides and determining their relative abundance. Peptides are isolated from control and thyroid hormone (TH)-treated retinas. Control and treated peptide pools are separately labeled with isotope-coded affinity tag (ICAT) reagents. The ICAT reagents contain biotin, which allows the peptides to be isolated via avidin affinity. The peptides from TH-treated retinas are labeled with ICAT reagents that are 9 Da heavier than the reagents used to label peptides from control retina. The heavy and light isotopes of the ICAT label differ only in that the heavy isotope contains 9 deuterium ions while the light isotope contains hydrogen atoms. This allows the peptides to be identified in mass spectrometry, where their peaks appear 9 Da apart. Identification of these doublets also allows the relative abundance of each peptide to be determined (Figure 2 is an example of this type of spectrum). Concurrently, the peptides are sequenced by mass spectrometry (Figure 2) and searched against protein databases to determine the protein the peptide came from.

to the manufacturer's recommended protocols using kits supplied by Applied Biosystems Inc., Foster City, CA. Control and treated retinal homogenates were solubilized in 0.1% SDS, 6 M urea, and protein quantification was performed using Bio-Rad's Protein Assay Dye Reagent Concentrate (Catalog number 500-3006). ICAT-labeled samples were then prepared using a Cleavable ICAT Reagent (Applied Biosystems, Bulk Kit Product No. 4337339), which specifically reacts with cysteine sulphydryls leaving an attached biotin group. Briefly, to equal amounts of control and TH-treated protein samples (100 μg), 80 μl of 25 mM ammonium bicarbonate buffer, pH 8.5 and 2 μl of 50 mM TCEP (Tris[2-carboxyethyl]phosphine hydrochloride) were added to enable full disulfide reduction. This reaction was allowed to proceed for 15 min at 37 °C, followed by addition of the appropriate ICAT reagent in 20 μl of acetonitrile. The latter reagent was allowed to react for another 2 h at 37 °C in the dark, whereupon light and heavy labeled samples were combined prior to digestion with 20 μg of chemically modified porcine trypsin (Promega, Madison, WI). Proteolysis occurred for 18 h at 37 °C, in 600 μl of 25 mM ammonium bicarbonate buffer, pH 8.5. Excess reagents were removed using an ICAT™ Cation Exchange Buffer Pack and Cation Exchange Cartridge (Applied Biosystems) and biotin-labeled ICAT peptides were isolated by avidin affinity column chromatography using an Affinity Buffer Pack (Applied Biosystems). The biotin group was finally cleaved from eluted peptides using 95% TFA containing 5 μl of a proprietary scavenger. Reaction was allowed to proceed for 2 h at 37 °C. Samples were stored as lyophilized powders.

ICAT two dimensional liquid chromatography tandem mass spectrometry: Liquid chromatography systems (UltiMate gradient pumps, SwitchOS II and FAMOS Auto-sampler; LC Packings/Dionex, Amsterdam, The Netherlands) were controlled by Applied Biosystems Analyst software during the data collection. The ICAT-labeled samples were brought up in 40 μl of 5% acetoni-
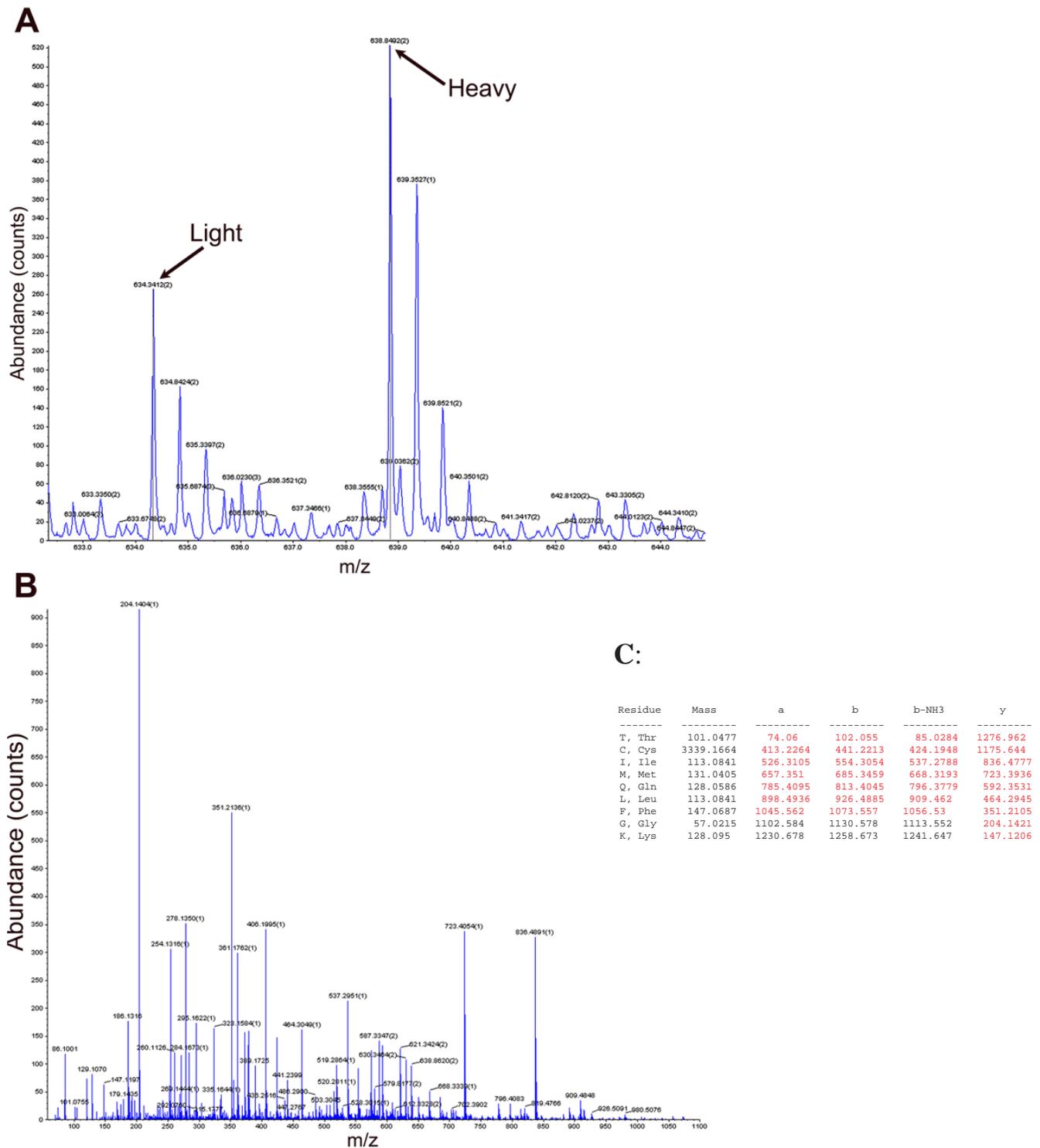
Figure 2. Mass spectra for the long-wavelength sensitive cone opsin, which increased in abundance during thyroid hormone treatment. **A**: Time-of-flight MS spectrum of isotope-coded affinity tag (ICAT) labeled peptides including light (D0) and heavy (D9) versions of the ICAT molecule. The difference in abundance between these peaks indicated that long-wavelength sensitive (LWS) opsin was 1.9 fold more abundant in the peptide pool from thyroid hormone-treated retinas, which was labeled with the heavy isotope of the ICAT molecule. **B**: MS/MS spectrum used to predict the sequence TCIMQLFGK. ProICAT software identified the protein as LWS opsin and these nine amino acids are an exact match to the peptide predicted from rainbow trout cDNA (AAM17921). The spectrum was validated by manual analysis. **C**: Ions observed in the spectra of **B** are highlighted in red.

TABLE 1. PREVIOUSLY CHARACTERIZED PROTEINS WHOSE ABUNDANCE WAS CHANGED DURING THYROID HORMONE TREATMENT IN RAINBOW TROUT RETINA

Avg T:C	Name	Accession ID	Peptide	Best conf	Score
27.914	Dissimilatory sulfite reductase subunit A	gi|20501973	IKCAGCPDDCVASVAR	50	16
24.369	Similar to double homeobox protein	gi|30154764	NAAPGGVSPCSLVGR	75	20
19.306	MLH1	gi|13517948	GEALCSISYVAR	75	20
19.306	Flavodoxin reductases	gi|48785221	AANQTICVCCSR	75	20
19.306	Leucyl aminopeptidase	gi|23475436	AAYVCGHVPVPR	75	22
15.033	Ubiquitination factor E4 (AAK33012, AY029484) omyk-59242	gi|20384666	ECSFDSDNFK	50	15
14.617	Probable RNA-directed DNA Polymerase	gi|7484429	DVCFRAAAHGGIALVDIK	50	16
14.320	Hyperglycemic hormone CHH-B	gi|1078947	TLCLVVVMVASLGTSGVGGRSVEGVSR	50	16
14.320	ATPase, E1-E2 type family	gi|22326934	EGEGIIGAIAISDCLRQDAEFTVAR	50	16
12.225	G-2 and S-phase expressed 1 (GTSE-1)	gi|20127556	AVGSPLCVPARR	50	18
11.057	Cyclin I [Q9Z2V9] ssal-10026	gi|9296967	AQMDSSQLIRCR	50	18
10.783	n-acylaminoacyl-peptide hydrolase (NP_036632, NM_012500) omyk-63225	gi|6978512	ILVSCPQGSR	75	23
10.570	Putative ankyrin protein	gi|12039395	CLCKHK	50	16
9.595	AGR_L_3383p	gi|15891808	LSGHCRGGFFPAIDADGR	75	20
9.524	Tissue inhibitor of metalloproteinase 2 (NP_035724, NM_011594) ssal-5300	gi|31543867	RADSSCSWYR	50	16
9.365	Histone macroH2A1.1 (AAC28846, AF058445) ssal-11335	gi|3395780	TVKNCLALADEK	75	20
8.973	Wpkci	gi|13365599	LCILGGR	50	16
8.928	Transposase (AAL93203, AF486809) omyk-55976	gi|19698551	QCLQCFAHTLQLVVGDGLK	50	16
8.368	Growth differentiation factor 5 precursor	gi|4262327	TSQVKLFSCSTNR	75	23
7.858	E1B protein, large T antigen	gi|1046213	CVCGK	50	16
6.523	ABC-type transporter homolog	gi|11356557	CAAPDLAPGTGTIGKVTAHDPR	50	18
6.331	Fatty acid synthase	gi|1345958	CPDLDYFVVFSSVSCGR	75	20
5.736	Citramalate synthases	gi|23101987	ICAVLGR	75	20
5.359	Alpha-2-HS-glycoprotein precursor (Fetuin-A)	gi|231467	LILFFCLAQLWGCR	50	16
5.295	Similar to ethanol induced 6	gi|27708440	NCRPSR	50	15
4.542	emb	gi|8953752	IGKDCHLGLMK	75	25
4.194	Long chain fatty acyl CoA synthetase	gi|11466137	LTDAQHAECCNWYDGPTILQR	50	16
4.097	Cytochrome P450 3A27 (O42563) omyk-66606	gi|5921919	VCGYYLGR	50	16
3.923	ps20 WAP-type four-disulfide core domain protein	gi|10198227	CPPPPRTLPPGACQAAR	75	22
3.786	F-box protein family	gi|15231601	CLCNVLKR	50	16
3.652	AtaPKS3 protein	gi|28170706	CAARFPAFGEALTVASASASGAVGIAVGR	50	18
3.611	Pyruvate dehydrogenase	gi|1200524	RNPLDC	50	16
3.157	RB118	gi|22726343	VVCLHRIGR	50	16
2.994	NADH dehydrogenase subunit 8	gi|11466585	LCEAVCPAQAITIETESR	50	15
2.989	Immunoglobulin VH domain	gi|4583873	LQESGGGLVQTGASLRLSCVASGR	50	16
2.974	Probable transposase	gi|7521506	ACLGLLSLARR	50	18
2.770	Phosphotransferase	gi|9628791	ECVFKSLLICNSVCLNHK	50	18
2.718	Solute carrier family 25 member 5 protein (AAM34660, AF506216) ssal-19916	gi|21105432	AGAREYNGLADCL	50	16
2.660	elongin C; transcription elongation factor B (SIII) (NP_005639, NM_005648) omyk-62584	gi|5032161	TYGGCEGPDAMYVK	50	18
2.549	RH2 opsin	gi|30578194	GCMLATVGMK	75	24
2.337	flavocytochrome c flavin subunit, putative	gi|24374580	LGACAVAEGVVTGRNAGR	50	18
2.175	Unknown omyk-43180		ALACCAYGGK	75	25

TABLE 1. CONTINUED.

2.135	Similar to AT motif binding factor 1	gi|27659206	HNICKGR	50	16
1.938	LWS opsin	gi|20269378	TCIMQLFGK	99	39
1.934	Olfactory receptor MOR256-21	gi|18480540	LPFCPHHQVDDFVCEVPALIR	75	20
1.922	Calreticulin	gi|1009712	SGSLFDNVLICDDPDYAKK	50	18
1.813	Putative nuclear protein, with a coiled coil domain	gi|17506383	ALCNVASRPR	50	17
1.807	4-Diphosphocytidyl -2C-methyl -D-erythritol synthase	gi|22298148	TAEQVLIHDGARCLATPDLINR	50	15
1.806	Glycosyltransferase GtfE	gi|11263653	EDCFAIGEVNQQVLFR	50	16
1.794	Secreted gel-forming mucin	gi|28865869	SPVTAPMTMSTSASAVTTSGCR	75	24
1.767	Polymorphic antigen P150 precursor	gi|7494470	CTSIQFHFDNYLK	75	22
1.753	Proteasome regulatory non-ATP-ase subunit 5	gi|18463069	ELEDHAECAAFSPATKLADR	50	16
1.753	Uridylate kinase	gi|48764614	GIQVCLVIGGGNIFRGISTAAK	50	16
1.723	Putative transcription factor BOFH	gi|584851	QACYKPLVDIACR	90	30
1.723	Putative nuclear protein, with a coiled coil-4 domain, nematode specific	gi|17539774	SAISDCVVSIRSSR	75	26
1.714	Transposase (CAB51372, AJ249085) omyk-64012	gi|5579035	EFSLSMC	50	18
1.707	Deoxyribonuclease	gi|9629863	ALVRACCVPPGDLPTPDGLADGGGR	50	17
1.665	Calcium channel, voltage-dependent, alpha 1H subunit	gi|10864077	LLCRQEAVHTDSLEGK	50	16
1.637	Transposase	gi|15890093	ACLGIIRLVK	75	20
1.636	Neural cell adhesion molecule 1	gi|18859063	FFLCEVVGDAK	75	22
1.621	RacP67PHOX COMPLEX, Chain A	gi|11513661	HHCPNTPIILVGTK	90	30
1.619	Similar to creatine kinase, mitochondrial 1	gi|28856248	HNNCMASHLTPAVYAK	99	54
1.605	WAP-type "four-disulfide core" and thyroglobulin type-1 repeat and antistasin family and Kunitz	gi|17538590	CVLNPKTEMGICCHQK	50	15
1.585	Glycosyl transferases group 1	gi|17555286	CVGFLEGLCGK	50	16
1.582	CG15199-PA	gi|24641213	LECTDDYLLLIR	75	21
1.582	3',5'-cyclic-GMP phosphodiesterase	gi|108470	VFHLSYLHNCETR	99	40
1.575	Tudor repeat 2 protein	gi|38259208	SCTQCPQIGDPCIVR	75	20
1.568	Omyk-23419	gi|22001927	CFIVGADNVGSKQMQAIR	75	20
1.565	Ornithine decarboxylase	gi|17432156	IIYAHPCK	75	22
1.561	3-hydroxyisobutyryl-coenzyme A hydrolase	gi|15239206	LDVIDRCFSR	50	16
1.529	SWS2 opsin	gi|30578192	SCMMNLLGLK	90	28
0.676	Putative gag-pol polyprotein	gi|37533472	CLHCKK	50	18
0.676	Oxysterol-binding protein-like protein OSBPL6	gi|17529995	ACLPAPCPDTSNINLWNILR	75	21
0.672	RNA polymerase beta-subunit	gi|21702604	ACIAGHIGIMR	75	20
0.656	Phosphopyruvate hydratase	gi|105934	ACNCLLLK	75	22
0.656	Putative nuclear protein family member, with a coiled coil-4 domain	gi|17551954	LCGFECTNVR	75	25
0.656	Similar to Cation transport protein	gi|13473049	SLCVYSFVHRGTR	50	16
0.656	Highly similar to triose phosphate isomerase	gi|16801613	SSTSADANETCAVIR	75	23
0.654	Solute carrier family 25	gi|16758854	CLLQIQASSGKNK	90	31
0.654	bsr5197	gi|27380308	ITGSSICDPLTSALPR	75	20
0.646	Upstream binding factor 1	gi|20955326	CYGRVTGTSK	50	16
0.642	Cytochrome P450	gi|21449376	ACIGRPFALQEATLVLALVLQR	50	16
0.639	1a protein	gi|20087045	LWAIAGCDGR	75	22
0.639	Similar to immunoglobulin heavy chain variable region	gi|27669594	LTLGVCIPDVISRDLK	75	25
0.636	Group IIF secreted phospholipase A2	gi|6174881	NSILSFVGYGCYCGLGGR	50	15
0.633	dynamin-like protein MGM1	gi|485546	NKCHSTIEK	50	16
0.626	methyl coenzyme M reductase system, component A2 homolog	gi|15678482	SPSPGFNQRSCGGR	50	16
0.621	Arrestin	gi|2308986	CAVEFEVK	75	24

TABLE 1. CONTINUED.

0.615	26L protein	gi|12085009	CTNDISSFLSEYK	50	16
0.611	yhbA	gi|10955525	EVPAKWACIHK	75	20
0.610	60S ribosomal protein L37	gi|1350736	CSACAYPAARLR	50	16
0.610	Unknown (protein for MGC:59412)	gi|28913682	RALLPPAACCLGCLAER	50	16
0.599	similar to proteasome subunit, α type 5	gi|20847133	IVEIDAHIGCAMSRLIADAK	75	22
0.597	PxORF80 peptide	gi|11068083	LVFEEETCKDQIMSR	75	20
0.592	β tubulin	gi|10242162	EIVHLQAGQCGNQIGAK	99	65
0.592	Rhodopsin	gi|10720158	WIVVCKPISNFR	99	48
0.592	Myosin heavy chain	gi|2104553	TYSGLFCVVVNPYK	75	21
0.590	guanine nucleotide-binding protein, β-4 subunit	gi|11055998	LLLAGYDDFNCNVWDTLK	90	32
0.588	Oxidoreductase, aldo	gi|15643766	GPEVSAIGLGCMR	75	20
0.587	bikunin	gi|17566852	AAKCPGDHVCTPR	50	18
0.586	Uridylyltransferase	gi|17934262	ADGSGIDCARR	75	23
0.580	SOX-20 protein	gi|4186021	SSGAGPSRCGQGR	50	18
0.577	7 transmembrane chemoreceptor family member	gi|17566844	GLIDMFRCHK	50	18
0.577	Pantetheine-phosphate adenylyltransferase	gi|28493532	GLLVDCCK	75	22
0.574	Quercetin 3-O-methyltransferase 1	gi|24212064	YLTKNQDGVSIAALCLMNQDK	75	20
0.570	Thyroglobulin	gi|13591876	DNFACVTSDQEEDAVDSLK	50	18
0.567	CG6562-PB	gi|18497296	IVACGANYGVFHASNGQVLR	50	16
0.566	Diadenosine tetraphosphatase	gi|15615408	TAYYVPGNHCNKLYR	50	16
0.551	(S)-2-hydroxy-acid oxidase chain D	gi|30019448	NTNEVAEVLKVCNTHK	50	18
0.551	Δ A	gi|18858541	NNRYVCACVSGYGGR	75	20
0.551	3-methyladenine DNA glycosylase	gi|46164618	FVDAAFAAFCTRNPLR	50	16
0.551	Undecaprenyl-PP -MurNAc-pentapeptide -UDPGlcNAc GlcNAc transferase	gi|33866863	LLGRFCGAVAVGLPAAAGR	50	16
0.526	Hyaluronan and proteoglycan link protein 3	gi|30102948	YPVVHPHPNCGPPEPGVR	90	28
0.525	Major royal jelly protein 2 precursor (MRJP-2)	gi|20138892	WLFMVACLGIACQGAIVR	50	18
0.518	exo-1,4-beta glucosidase	gi|1016746	CVEHEVSEAQAAIITIGRQAGEGLDR	75	20
0.517	ATP-dependent DNA helicase	gi|21233561	IRGDGADGLTICTFHALGLK	75	24
0.513	ATP-dependent DNA helicase	gi|15924217	VGRSDQQSYCVLIASPK	75	26
0.503	AP2 domain protein RAP2.2	gi|18400321	MCGGAIISDFIPPPRSLR	50	17
0.503	Clusterin precursor (P14018) ssal-1835	gi|1705937	CVAIQDIDCSGKKPLTGPLK	50	16
0.501	P0686C03.10	gi|28201266	ENPGVVSEALFALSCGPDLRVK	50	16
0.498	transcriptional regulator, MerR family	gi|21229272	IEGILQGACR	75	20
0.487	C20orf92 protein	gi|18592788	RPCPSPEPGGR	50	16
0.485	β tubulin	gi|1220547	GHYTEGAELIDSVLDVCR	99	66
0.472	CG14768-PA	gi|20129709	CPSPGLRPEPQSPTIARPQK	50	16
0.468	Protease subunit of ATP-dependent Clp proteases	gi|48849255	VSTVCIGQAASMGSFLLAAGEPGMR	50	16
0.459	876aa long hypothetical DNA-directed DNA polymerase	gi|15921715	AVCKLYDK	50	16
0.424	Unknown omyk-43142		VKMCIYLR	50	18
0.418	Yts1F protein [Yersinia enterocolitica (type 0:8)]	gi|27529238	CAIKYWR	50	16
0.414	acetyltransferase, GNAT family	gi|16126448	MRINACWPLGAPDR	50	16
0.409	Unknown omyk-41466		IGALGCLCSDVSRLVK	50	16
0.379	Recombinational DNA repair ATPase	gi|23469354	CQVFITCVDQEFLR	75	24
0.367	ferredoxin-like protein	gi|39648848	LACQCFVR	50	18
0.362	UDP-glucose 4-epimerase	gi|23104908	NGSAESLARVAAICGR	75	20
0.352	NAD-dependent aldehyde dehydrogenases	gi|23472045	CWIEAGLPAGVLNLLQGGR	50	15
0.337	Zinc finger protein 304 (XP_065054, XM_065054) ssal-18954	gi|27500786	IHTGERPYGCEVCGR	50	16
0.302	Probable transport transmembrane protein	gi|17545137	ASLWLDRVSGCIFIGLGLR	50	16
0.295	Fibroblast growth factor receptor precursor	gi|596009	KPLKGQTDGYIVVYCLK	50	18

TABLE 1. CONTINUED.

0.291	Similar to hypothetical protein FLJ38281	gi|20864596	CVVCREAFPNAVALR	75	24
0.287	Polyprotein	gi|1030731	SNVTCYRCGQPGHFSNQCPK	50	16
0.286	Peroxiredoxin 2 family protein	gi|15676839	AQESVAIFTKPGCQFCAK	50	18
0.268	3-oxoacyl-(acyl-carrier-protein) synthase II	gi|17548579	LACPLPAFEVPATYPR	50	18
0.264	Muscarinic receptor 5	gi|18409573	ALLRSCFSCPHPTLVQR	50	17
0.264	lysozyme	gi|11342495	ISQEGLEHLIDCEGCKR	50	15
0.261	Arginine decarboxylase	gi|17224235	IGLEAGSKPEILMAMGCLCK	75	22
0.251	Unnamed protein product (BAB31871, AK019829) oner-29064	gi|12860185	TCLAGFSPDGLLNVCQR	50	18
0.242	Inner mitochondrial membrane peptidase 2-like	gi|16716421	CFKAFCK	50	16
0.238	Adenylosuccinate synthetase	gi|18976680	CAIIEPKHK	50	17
0.237	Germination protein	gi|23097938	SNEIAINGLLDGYCLLIK	50	16
0.237	a372L	gi|9631940	LYIRGMCR	50	16
0.227	Similar to 60S ribosomal protein L9	gi|27715587	QAVLCLPPGCALRALGR	50	16
0.225	inositol 1,4,5-triphosphate receptor 2 (NP_064307, NM_019923) ssal-9833	gi|9910290	CVVQPDAGDLANPPKK	50	15
0.209	Lipid transfer protein	gi|21591782	CLVGAANSFPTLNAAR	50	16
0.208	Envelope protein E1	gi|402450	HQTVQTCNCSLYPGHVSGHR	75	20
0.202	LmbE homologs	gi|23104913	GPRTSNCAIPSAAPIANTR	50	16
0.201	Ring finger protein 150	gi|51464218	LACDPNTKFAAPTR	50	16
0.185	Histidinol-phosphate aminotransferase	gi|14520265	GILVRDCTSFGLPGYIR	50	18
0.185	Nucleic-acid-binding protein containing a Zn-ribbon	gi|48780774	ALCSECQSLDLNWLDSDRR	75	20
0.182	Dimethyladenosine transferase	gi|46192173	DARCLPALAEVAAAWPGR	75	22
0.180	Arp2	gi|11359368	VVEVAGLGCIGR	50	18
0.179	Guanylate nucleotide binding protein 5	gi|23956350	CFVFDAPALGSK	50	15
0.174	hypothetical protein MGC28149 (NP_666301, NM_146189) omyk-23548	gi|22122731	AINPLGEDVVECTLLVR	75	21
0.174	pyruvate kinase	gi|15789598	FRPSVPVVCATPSHDVR	75	26
0.172	IgiA	gi|5852323	LCAEQALAALPLTAAVLGR	50	19
0.170	enterobactin synthetase, component D	gi|17988425	GCAIAVAARQSR	75	22
0.167	Phytochrome A type 3 (AP3)	gi|130181	YACEFLAQVFAVHVNR	50	19
0.164	NADPH--ferrihemoprotein reductase (A28577) omyk-57898	gi|85592	EQGKEVGETVLYCGCR	75	22
0.159	Dual specificity phosphatase and pro isomerase domain containing 1	gi|51491914	ALSDDHSKILVHCVMGR	50	16
0.144	Cytosine-5-methyltransferase 3-like protein isoform 2	gi|28872780	NCFLPLREYFK	50	18
0.138	Hypothetical protein	gi|22980883	VVCNNTLQIALGR	50	16
0.129	Envelope glycoprotein	gi|13559470	CVTPNCTDWK	50	16
0.125	Similar to Protein kinase PKX1	gi|30155809	EVIRPFLICVLK	75	24
0.124	β-globin (BAA11632) omyk-21057	gi|1183021	LLADCITVCVAAK	75	20
0.120	Phosphoenolpyruvate synthase	gi|21231605	LCAENGGGEVAVAVR	50	16
0.118	Similar to heparan sulfate 6-O-sulfotransferase 2 isoform S	gi|27707418	ITAASAGGLEDSSFLCR	50	16
0.116	Putative Na+-dependent inorganic phosphate cotransporter	gi|4895179	CAAEGVLTGGGGSEAIAEVR	50	16
0.110	β-tubulin	gi|4210476	GRSCTVQAGQCGNQIGAK	75	22
0.104	protein kinase C-zeta-interacting protein	gi|27462493	AGVCTGFKCHK	75	22
0.096	GTP-binding protein -related	gi|15222829	CFSSKVSMSLK	50	16
0.081	Insulin receptor-related receptor precursor	gi|112516	CVTAESCANLRSVPGR	50	15
0.071	c-myc gene single strand binding protein 2 omyk-46240	gi|4506447	CDAVIAHFNGKFIK	50	16
0.061	T-complex protein 1 gamma subunit	gi|6318665	IEKIPGGAIEDSCVLEGVMFNK	50	18

TABLE 1. CONTINUED.

0.060	Non-selenium glutathione phospholipid hydroperoxide peroxidase (CAB65456, AJ243849) ssal-71537	gi|6689393	CVFVIGQDK	50	18
0.055	Thioredoxin reductase	gi|48787275	IGSLPNVSLCTR	75	26
0.053	Unknown ssal-68895		TGCHLVAGR	50	18
0.050	chloroplast protein-translocon-like protein	gi|13937285	CPVSVSLIAR	75	21
0.047	Unknown ssal-28398		LVYIVCCK	50	16
0.040	KIAA0296 gene product (NP_055514, NM_014699) omyk-42104	gi|41281441	QLSSHICAHLR	50	16
0.040	Unknown ssal-13231		VFCCSLVR	50	18
0.028	Unknown omyk-49337		CHPLLRCSPR	50	16
0.005	hypothetical protein DKFZp762C1110.1 (T47158) ssal-8353	gi|11360273	CVGHNGRTLAHESCNPK	50	18

Previously characterized proteins that were quantified and had greater than 50% change in expression level after thyroid hormone (TH) treatment. We report a T:C ratio, where T represents the abundance of the peptide in TH-treated retina, and C represents the abundance in the control retina. A T:C ratio represents the fold increase (if >1) or fold decrease (if <1) of the reported peptide in the retina of trout treated with TH. For proteins represented by multiple peptides (Table 3), the average fold change of all peptides is presented in brackets. Best confidence ("Best conf") and "Score" are indices that represent confidence in assigning mass spectrometry results to particular peptides, as defined in the Methods.

trile/water containing 0.1% formic acid and loaded into autosampler vials. A 10 μl volume was loaded onto a 100 μl sample loop with the remainder of the volume being filled with 0.1% formic acid. The SwitchOS II loading pumps were set to a flow rate of 30 μl/min, and the sample was pumped onto a 500 μm x 15 mm BioX-SCX 5 μm strong cation exchange column connected, in turn, to a 300 μm x 1 mm PepMap C18, 100 Å nanoprecolumn (LC Packings/Dionex). The eluant from these columns was allowed to divert to waste for 7 min using the SwitchOS II. The SCX column was switched off-line and
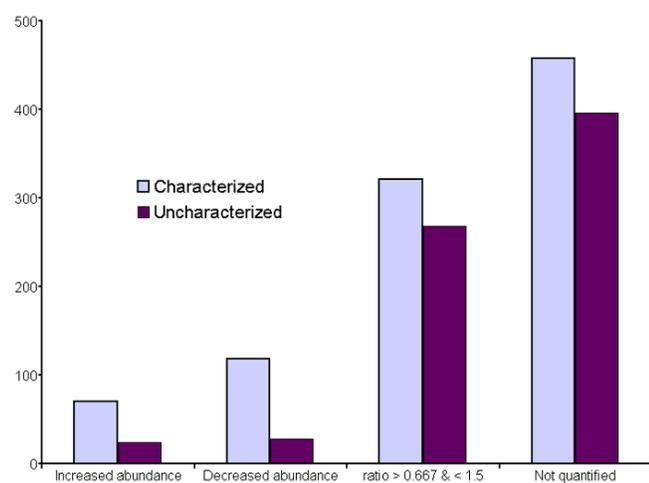

Figure 3. Detection of peptides in thyroid hormone and control retinas. A total of 1683 peptides detected. They were classified as increased or decreased in abundance during thyroid hormone (TH) treatment if the relative abundance between TH and control differed by 50%. Proteins were also grouped into those that have been described previously and those that have not. Peptides designated as "not quantified" were not assigned relative abundance ratios or were detected in only one of the two peptide pools.

the sample was washed for another 7 min on the abovenamed PepMap™ C18 column to concentrate and desalt the peptide mixture before MS analysis. The eluant was then diverted to the UltiMate pumps, and the sample was eluted onto a 75 μm inner diameter (I.D.) x 15 cm PepMap™ 3 μm, 100 Å C18 nanocolumn (LC Packings/Dionex). The column was sleeved via 20 cm of 20 μm I.D. fused silica (Poly Micro Technologies, Phoenix, AZ) to a Valco stainless steel zero dead volume fitting which had the high voltage lead (2500 V) and a New Objective (Woburn, MA) emitter fused silica tip positioned at the orifice of a PE SCIEX API QSTAR Pulsar in positive ion mode (PE SCIEX, Concord, Ontario, Canada). The UltiMate pumps were set to deliver a flow rate of 150 nl/min with the following buffers: solvent A: 0.1% formic acid/water; solvent B: 80% acetonitrile/20% water/0.1% formic acid. The gradient used to elute the peptides was 15 min at 0% B, 30 min to 60% B, 3 min to 80% B and held for 2 min, 3 min to 0% B, and 8 min to re-equilibrate the column. The SCX column was then switched back in-line with the SwitchOS II buffer of 0.1% formic acid/water to equilibrate for the next injection.

To elute further peptides from the SCX column, 50 μl volumes of 0.5% formic containing from 100 to 1000 mM ammonium acetate, pH 4.0, was applied successively in 100 μm increments, finishing with a 2 M solution. The above described organic modifier gradient was then applied after each salt injection.

The mass spectrometer information-dependent acquisition parameters were as follows: After a 1 s survey scan from 300-1500 m/z peaks with signal intensity over 10 counts with charge state 2-5 were selected for MS/MS fragmentation using a software determined collision energy and then a 2 s MS/MS from 65-1800 m/z was collected for the two most intense ions in the survey scan. Once an ion was selected for MS/MS fragmentation it was put on an exclude list for 180 s to prevent that ion from being gated again. A 6 amu peak window

was used to prevent gating of masses from the same isotopic cluster during the survey scan.

The software used to analyze the data was ProICAT SP2 (Applied Biosystems software is version 1.1). The National Center for Biotechnology Information (NCBI) non-redundant database was searched with an error tolerance of 0.15 Da for both the MS and the MS/MS scans. Also searched were databases provided by the Genomic Research on Atlantic Salmon Project (GRASP). The results were then written by the software to a Microsoft Access database. The results database was then queried with a minimum confidence limit of 50 and a score of 15. The number of sequences in the databases at the time searched was 1,934,002 for NCBI, 13,352 for the *Salmo salar* GRASP, and 19,509 for the *Oncorhynchus mykiss* GRASP databases. The only fixed modification considered was the cysteine ICAT labels, MS and MS/MS tolerances were set to 0.15, and one missed cleavage was permitted. Nontryptic peptides were not considered.

Experimental and control proteins were labeled independently and subsequently mixed together. Therefore, both heavy and light protein adducts are digested under exactly the same conditions and resultant peptides measured relative to one another. Under these circumstances, any variation in proteolytic digestion would be observed in both heavy and light forms and thus be irrelevant. Moreover, control and experimental peptides were separated under identical LC and MS separation conditions. As such, relative measurements were reliably obtained and the major source of error can be attributed to biological variation of the proteome.

The Interrogator peptide database search algorithm of the ProICAT 1.0 SP2 software (Applied Biosystems, Foster City, CA). For each database peptide, within tolerance of the observed parent mass, the algorithm rapidly counts the theoretically expected ions found in the spectrum. The score reported for each database peptide is the sum of intensity-based weights for all matching fragments. From the distribution of top scores for a particular spectrum, a score deemed representative of the best random peptide hits is found, and a distance score is computed as the difference between the top peptide score and this best random score. Discriminant analysis of score, distance score, and other metrics was performed on annotated data to determine a discriminant function that is effective at discriminating right answers from wrong. Identification confidence is reported based on the observed rate of correct identifications for various ranges of the discriminant function. Confidence is based upon both the score and distance score

and is dependent upon both the number of matching ions and the distance of the matched peptide from other matches for the same MS/MS data. Protein expression ratios are calculated from the MS spectra using an LC/MS spot-finding technique to detect and quantify the abundances of peptides. ICAT reagent expression pairs and isolated peptides are found. A quality value for each quantification result is computed for complete pairs based on the accuracy of the measured mass difference and the similarity of light and heavy isotopic profiles. Finally, ProICAT associated MS-based peptide expression measurements with MS/MS-based protein identifications to compute expression ratios for each protein.

The ICAT method has been intensively studied by a number of labs. When equal amounts of heavy and light congeners are analyzed by ESI-MS or MALDI-TOF MS one invariably obtains ratios of 1:1, within pipetting and instrument error [69]. Indeed this criterion of performance is monitored whenever a new stable isotope procedure is evaluated.

In our results, the protein accession number and name represent the raw software output. Other proteins that contain the exact peptide described, including those from other species, are equally likely to represent the actual protein that was detected in the trout retina. The peptides reported in the results section can be searched against protein database (e.g., NCBI's protein-protein BLAST) for alternate proteins that contain the peptide.

RESULTS

We demonstrate that ICAT combined with 2D LC-ESI-MS/MS is a rapid method to compare the relative abundance of proteins between two retinal samples. Consistent with previous reports [75-77], we find that the technique provides broad coverage of the proteome. In addition, previous reports detailing the performance of the University of Victoria Genome British Columbia Proteomics Center indicated a strong correlation between the relative abundance of proteins reported by ICAT combined with LC-ESI-MS/MS, and results of western blots or 2-D gels [74,76].

We found that fractionation of the sample led to greater coverage of the proteome, as compared to our preliminary experiments, where fractionation of the samples was not employed.

A D9:D0 ratio (Heavy ICAT isotope: Light ICAT isotope), differing by the inclusion of 9 deuterium ions in the heavy isotope, (Figure 1) greater than 1.0 represents peptides that were more abundant in the TH-treated retina, and ratios less

TABLE 2. SUMMARY OF THE NUMBER OF PEPTIDES DETECTED DURING THYROID HORMONE TREATMENT IN RAINBOW TROUT RETINA

Type of protein	Up regulated (ratio>1.5)	Down regulated (ratio<0.667)	Ratio>0.667 & <1.5	Total quantitated	Not quantitated	Singlet identified	Total
Characterized	70	118	321	509	371	87	967
Uncharacterized	24	28	268	320	359	37	716
Total	94	146	589	829	730	124	1683

Statistics on all peptides detected. Peptides affected by thyroid hormone in the retina of rainbow trout that changed more than 50% in their relative abundance (ratios >1.5 or <0.667) were considered significant.

TABLE 3. ASSESSMENT OF ICAT/MS TECHNIQUES REPRODUCIBILITY BY ANALYZING DIFFERENT PEPTIDES THAT WERE IDENTIFIED FROM INDIVIDUAL PROTEINS

Name	Number peptides detected	Accession ID	Peptide	Conf	Score	T:C	Avg T:C	St Dev
β tubulin	5	gi|13324679	LTTPTYGDLNHLVSATMSGVTTCLR	99	50	0.968	0.833	0.152
			MREIVHLQAGQCGNQIGAK	99	42	0.947		
			TAVCDIPPR	99	48	0.867		
			NMMAACDPR	90	33	0.791		
			EIVHLQAGQCGNQIGAK	99	65	0.592		
Transferrin	5	gi|5837759	SHNEPYYDYAGAFQCLK	75	24	1.134	1.011	0.087
			CLVEGAGDVAFIK	90	34	0.994		
			ETNNCDFTTYFSK	50	16	0.985		
			CHDLAANVAQFSCVR	99	51	0.929		
			IECQDAPTVDECIKK	99	36			
Glycogen phosphorylase, brain form	4	gi|1730559	SSKFGCR	50	16	1.471	1.083	0.267
			TCAYTNHTVLPEALER	99	40	1.050		
			INMAHLCVIGSHAVNGVAR	99	36	0.919		
			QLLNCLHIITLYNR	90	30	0.894		
α-tubulin	4	gi|340019	CDPGHGKYMACCLLYR	90	31	1.128	0.941	0.128
			AYHEQLSVADITNACFEPANQMVK	90	34	0.865		
			SIQFVDWCPTGFK	90	32	0.919		
			YMACCLLFR	75	22	0.853		
Similar to guanine nucleotide binding protein	3	gi|27881927	LFVSGACDASAK	99	42	0.598	0.583	0.018
			LLLAGYDDFNCNVWDTLK	90	32	0.588		
			ADQELMVYSHDNIICGITSVAFSK	99	38	0.562		
Pyruvate kinase	3	gi|21038972	AGKPITCATQMLESMIK	99	38	0.987	0.912	0.068
			AEGSDVANAVLDGADCIMLSGETAK	90	31	0.896		
			NTGIICTIGPASR	99	46	0.853		
Sodium/potassium-transporting ATPase	3	gi|18858309	SSVTWVALARVAALCNR	50	16	1.205	1.107	0.138
			ACVIHGTDLK	99	46	1.009		
			CIELSSGSVK	50	17			
Phosphopyruvate hydratase β	3	gi|105934	SGETEDTFIADLVVGLCTGQIK	99	50	0.845	0.754	0.096
			VNQIGSVTESIQACK	99	52	0.764		
			ACNCLLLK	75	22	0.654		
Creatine kinase	3	gi|6016429	LGYILTCPSNLGTGLR	99	42	1.032	1.201	0.365
			VCAEARDQHK	75	22	0.951		
			HNNCMASHLTPAVYAK	99	54	1.619		
V-type ATPase B subunit	2	gi|4929105	TACEFTGDILR	99	44	1.002	0.942	0.119
			GPTVLAEDYLDIMGQPINPQCR	50	16	0.883		
EAA44879	2	gi|30177396	YMSCCLLYR	90	28	0.950	0.934	0.030
			SIQFVDWCPTGFK	90	32	0.919		
Cellular nucleic acid-binding protein	2	gi|29423610	DCEQTEDACYNCHR	50	18	0.986	0.935	0.102
			CGEIGHVAVQCSK	99	50	0.884		
Similar to phosphorylase phosphatase	2	gi|28422226	VKEFCENLPADGR	50	16	1.019	0.925	0.186
			LNIISNLDCVNEVIGIR	99	50	0.832		
RIKEN cDNA 3110065L21	2	gi|25072051	IHEGCEEPATHNALAK	99	42	0.955	0.866	0.177
			EDKLECSEELGDLVK	75	26	0.778		
Arrestin	2	gi|2308986	VYVMLSCTFR	75	25	0.690	0.653	0.075
			CAVEFEVK	75	24	0.615		
SI:bZ18K17.1	2	gi|22204199	GILLFGPPGCGK	99	42	1.068	0.967	0.203
			LGANSGLHIIIFDELDAICK	90	34	0.866		
Glutamine synthetase	2	gi|21666321	LVLCEVLK	90	29	0.941	0.903	0.077
			RPSANCDPYAVTEALIR	99	56	0.864		
Creatine kinase, testis isozyme	2	gi|125314	FCTGLTK	75	21	1.076	0.977	0.199
			GFCLPPHCSR	99	48	0.877		
Guanine nucleotide-binding protein G(I)	2	gi|121009	ELPGHTGYLSCCR	75	20	1.094	0.912	0.363
			LLLAGYDDFNCNIWDAMK	50	16	0.731		
Chain A, Structure of the RacP67PHOX complex	2	gi|11513661	HHCPNTPIILVGTK	90	30	1.621	1.228	0.786
			CVVVGDGAVGK	99	39	0.835		
Rhodopsin	2	gi|10720158	YIPEGMQCSCGIDYYTR	99	36	0.983	0.788	0.392
			WIVVCKPISNFR	99	48	0.592		

The table shows proteins that were identified multiple times from different peptides. The quantification of multiple peptides that may have originated from the same protein allow one to assess the reliability of the data. We report a T:C ratio, where T represents the abundance of the peptide in thyroid hormone treated retina, and C represents the abundance in the control retina. A T:C ratio represents the fold increase (if>1) or fold decrease (if<1) of the reported peptide in the retina of trout treated with thyroid hormone. The column labeled "Conf" is the confidence.

than 1.0 are peptides that were more abundant in the control retina. Standards run with this ICAT protocol at the University of Victoria Genome British Columbia Proteomics Center indicate that it can reliably detect a 30% change in protein abundance. We therefore chose a criterion fold change of 50% to represent a change in relative protein abundance during TH treatment. Similar to a previous study using this proteomics facility [76], we chose this criterion to be a 50% change in relative abundance. Therefore, a peptide met our criterion if the D9:D0 ratio was greater than 1.5 or less than 0.667. In our results the ratio D9:D0 is equivalent to T:C ratio, where T represents the abundance of the peptide in thyroid hormone treated retina, and C represents the abundance in the control retina. Our criterion is arbitrary; some proteins that do not meet it may still be changing in a measurable way that is biologically meaningful. The data in Table 1 and Appendix 1 are intentionally presented in order of the fold change for each peptide. Thus, one can quickly see which peptides are above or below a particular criterion. This proteomic approach serves as an effective tool to explore changes in a proteome and the regulation of individual proteins can be validated using other techniques if they are of particular interest. A peptide was considered "quantified" if a ratio was reported by the software. Other peptides were detected in only one of the two pools, and therefore no ratio is available. Still other peptides were identified but not quantitated. This could be due to incomplete labeling, low signal-to-noise ratios, and/or incomplete elution during fractionation or purification stages.

We further categorized peptides as belonging to proteins that were either "characterized" or "uncharacterized." Uncharacterized proteins represent results where the protein is unnamed or listed as "hypothetical" or "putative." Further uncharacterized proteins included those submitted to databases based on large-scale nucleotide sequencing, such as those beginning with the prefix "ENSANGP" or those identified by the RIKEN mouse cDNA project. Alternatively, we describe proteins as characterized if they have been named and their function described/predicted.

We also included as "characterized" all proteins that were

detected when the MS data were processed against the salmonid EST databases of GRASP. Some of these proteins are not named: however, we know that they are expressed in salmonids as mRNA that conceptually predict the exact peptides. For peptides found in the GRASP database, the name of the protein is followed by the unique GRASP identifier for the cDNA clone and the nucleotide accession number. The GRASP sequences comprise three salmonid species that can be discerned from their unique identifiers (ssal represents *Salmo salar*, Atlantic salmon; omyk represents *Oncorhynchus mykiss*, rainbow trout; oner represents *Oncorhynchus nerka*, sockeye salmon). For the genes from GRASP, the GenInfo Identifier (GI) number that is listed often represents a homolog of the gene from another species. For example, in Table 1, a peptide that is part of the protein cyclin I was increased 11 fold by TH treatment. The 12 amino acid peptide is an exact match to a cDNA from Atlantic salmon (*Salmo salar*). This cDNA has been identified, by sequence identity over its entire length, to be a homolog of the mouse cyclin I gene; thus, the mouse cyclin I gi number is listed. One may query the GRASP project for further details of individual cDNAs, including using the accession number we report to search their online database of gene sequences (GRASP) associated with their cDNA microarrays [78].

In this study, we detected 1,684 unique peptides, varying from 5 to 29 amino acids in length (Figure 3, Table 1, Table 2, Appendix 1). The results, when comparing TH-treated to control retina, suggest that 70 characterized proteins (Table 1), and a further 24 uncharacterized proteins (Table C in Appendix 1), increased by more than 1.5 fold. TH treatment led to a decrease in abundance of 122 characterized proteins (Table 1) and 24 uncharacterized proteins (Table C in Appendix 1).

We quantified many proteins that changed less than 50% in their relative abundance during TH treatment, including 321 characterized (Table A in Appendix 1) and 268 uncharacterized proteins (Table D in Appendix 1). The majority of peptides (i.e., 854) were not quantifiable or were detected in one sample only (Tables B and E in Appendix 1).

To assess the reliability of the technique, we examined multiple peptides that originated from the same protein to see if they changed in a similar manner. Nine proteins were detected more than twice (Table 3). These are reported along with the average and SD of the quantification for each peptide. Seven of these groups of peptides had minimal variation with standard deviations less than 0.16. Two others proteins have more variation among peptides, although the standard deviations remain small (<0.37) relative to our criterion (0.5).

Twelve proteins were detected twice, and are reported with the average and difference in the quantifications. The average of these differences (0.144) is small relative to our criterion (0.5). In one instance, the variation (0.786) is larger than our criterion. Until genomic sequencing is complete for rainbow trout we will be unable to eliminate the possibility that some of the peptides in Table 3 originate from different proteins. Thus, our data appear to be reliable en masse; however, each result should be interpreted with caution until it is confirmed with other methods.

TABLE 4. SUMMARY OF CHANGES IN OPSIN PROTEIN ABUNDANCE DURING THYROID HORMONE TREATMENT

Opsin class	Accession ID	Peptide	Avg T:C
LWS	gi|20269378	TCIMQLFGK	1.938
RH2	gi|30578194	GCMLATVGMK	2.549
SWS2	gi|30578192	SCMMNLLGLK	1.529
SWS2	gi|30578192	LATIPSCFSK	1.317
RH1	gi|10720158	YIPEGMQCSCGIDYYTR	0.983
RH1	gi|10720158	WIVVCKPISNFR	0.592
RH1 (SWS1?) opsin	gi|3914251	SSSLYNPLIYICMNKQSR	Detected only in control retina

Summary of changes in opsin protein abundance during thyroid hormone treatment. We report a T:C ratio, where T represents the abundance of the peptide in thyroid hormone treated retina, and C represents the abundance in the control retina. A T:C ratio represents the fold increase (if>1) or fold decrease (if<1) of the reported peptide in the retina of trout treated with thyroid hormone.

We have summarized the TH-induced changes to opsin proteins in Table 4. Changes were observed in four of the five opsin classes known to occur in rainbow trout [13] and other salmonids [79]. Four peptides from three cone opsins were unambiguously identified, as were two peptides from rod opsins. The expression of these opsins in particular photoreceptor classes has been accomplished using in situ hybridization [13] and immunohistochemistry [14]. Our results suggest that LWS and MWS opsins were more abundant (1.9- and 2.5 fold, respectively) in TH-treated fish. Two peptides were detected from SWS2 opsin, one of which met our criterion for increased abundance (1.5 fold) and the other showed similar levels but was increased only 1.3 fold. Peptides were also detected from the rod opsin gene RH1.

DISCUSSION

Effects of thyroid hormone in the retina: TH is known to have several effects in the retina. In *Xenopus*, TH leads to increased proliferation in the retinal margins [31,32]. A similar observation has been made via analyzing BrdU incorporation in rainbow trout retina [12]. TH treatment also leads to increased proliferation in other salmonid sensory epithelia, including coho salmon olfactory epithelium [80]. Our results suggest that TH may promote proliferation in the retina. Most notably, cyclin I increased with TH treatment (Table 1). This was supported by another peptide, G-2, and S-phase expressed 1 (GTSE-1), which increased in abundance. GTSE-1 is expressed specifically during cell cycle phases S and G2 [81,82].

TH is also known to affect the density of photoreceptors in the trout retina [20]. Our results indicated that peptides derived from various tubulin subunits changed in abundance during TH treatment. In particular, three peptides decreased in abundance. Ten peptides attributed to tubulins did not meet our criterion of 50% fold change and appear in Table 3 and Appendix 1. Microtubules are known to be involved in retinal mosaic formation [83], and tubulin regulation is important to zebrafish CNS regeneration and development [84]. TH has been implicated in regulating tubulin in other neural regeneration paradigms [85].

TH has recently been found to effect the optical transparency of the rainbow trout lens, probably through modulation of ocular sodium/potassium ATPases [86] which are modulated by TH in other salmonid tissues [87]. We detected three peptides of sodium-potassium ATPases (Table 3), none of which changed in abundance in an impressive manner.

Other known effects of TH in the retina include modulation of deiodinases [33] and changes in rhodopsin/porphyropsin ratios [27-30], although the pathways that regulate the latter, involving an unidentified 3,4-dehydrogenase, remain unknown. Two peptides similar to bacterial dehydrogenases, with unknown function in vertebrates, were increased threefold by TH; these might bear further exploration. We also know that TH affects opsin expression in the trout retina [12,14,17-20], discussed in the next section.

Opsins: The peptides reported by the ICAT software for the LWS and MWS cone opsins are identical to the amino acid sequence predicted from our cDNA clones [13]. Both opsins appear to be increased in abundance during TH treatment (Table 4). Similarly, both of the SWS2 opsin peptides are an exact sequence match to the protein predicted by our cDNA clone of the gene [13]. The difference in the results from the SWS2-derived peptides (1.3 and 1.5 fold changes were observed) was relatively small. It is a matter of interpretation and further investigation whether this increase in SWS2 opsin is biologically significant. A recent examination as to opsin mRNA levels after nine days of TH treatment (identical to the current methods) using quantitative real-time RT-PCR (QPCR) supports the conclusion that our TH treatment affected cone opsin gene expression [26]. The QPCR results are in accordance with those described here; the TH: Control ratio of transcripts was 0.77 for RH1, 2.1 for SWS2, and 1.7 for MWS (compare to Table 4). Only the ratio of LWS opsin transcripts differed from the current results, with TH having no apparent effect on LWS opsin transcripts.

Changes in visual sensitivity during TH treatment are also measurable and include a loss of sensitivity to UV light [13,14,17-19] and an increased sensitivity of the MWS cone mechanism [19], similar to results from natural development [37]. The TH-induced increase in sensitivity of the MWS mechanism is consistent with the MWS opsin peptide being the most increased opsin in the current results, with a 2.5 fold increase in MWS opsin protein abundance.

Two peptides were detected from the rod opsin gene, RH1. One was a perfect sequence match to the RH1 gene product predicted from cDNA [13] and apparently changed little with TH treatment (ratio=0.98). The other peptide, which decreased in abundance with TH treatment (ratio=0.59), only matched the predicted gene product in 10 of the 12 amino acid residues. Together, these results suggest that a second RH1 gene is expressed in the rainbow trout retina, as is the case with some eels [88,89]. Indeed, another salmonid, the ayu (*Plecoglossus altivelis*) possesses two RH1 genes, although only one copy has been isolated in the retina at the developmental stages that were examined [90]. Reduced RH1 expression (as measured by in situ hybridization) has been reported in early *Xenopus* embryos treated with TH and retinoic acid together, although not detectably with TH alone [91].

The only class of opsin not detected was SWS1 opsin, which is expressed in UVS cones [13,14]. It could be that there was effectively a complete lack of SWS1 opsin protein present after TH treatment. Our past analyses have detected minimal amounts of SWS1 opsin after TH treatment as measured by in situ hybridization and immunohistochemistry [12-14] as well as by QPCR [26]. If this were the case, SWS1 would not be detected by ICAT because the technique relies on detecting doublets of peptides (separated by 9 Da) in the MS spectra. In this context one peptide is intriguing: It was identified by the software as a singleton in the control retina, and thus was not detected in the TH-treated retina. It was identified RH1 opsin from the European eel (*Anguilla anguilla*, see Table 4). The *Oncorhynchus mykiss* RH1 cloned previously [13] predicts 15 of 18 amino acids in the peptide reported; however, it lacks a cysteine residue in this region and cannot be the source of the peptide, as the ICAT label binds

only to cysteine. The cysteine is also absent from this peptide in the RH1 opsins of other salmonids [79,92]. The SWS1 gene is the only opsin identified from trout that contains a cysteine in the 18 amino acids that share sequence identity with this peptide (SSCVYNPLIYAFMNKQFN). Perhaps a second SWS1 gene is expressed in the trout retina, similar to another salmonid [90]. Thus, this peptide may be a portion of the missing SWS1 opsin present only in the control retina, or as mentioned previously, there may be another copy of the RH1 gene to which this peptide can be attributed.

Other photoreceptor-specific proteins were detected, including two peptides from arrestin, which were decreased 0.69 and 0.62 fold (Table 1, Table 3).

Retinal development: Several peptides were detected that play a role in retinal development in other model organisms. These include ΔA (matching the sequence from zebrafish *Danio rerio* [93]), which was less abundant (ratio=0.55) in TH-treated retina, and ΔC (matching the sequence of a cDNA clone from Atlantic salmon, *Salmo salar*), which was also less abundant (ratio=0.73) but did not meet our criterion. The Δ-Notch pathway is involved in retinal cell fate decisions [94,95] including the spatial patterning of cone photoreceptors in zebrafish [96]. We also detected a peptide from Notch2 (matching the sequence from pufferfish, *Takifugu rubripesi*; Table B in Appendix 1), but no quantification was available.

We detected retinoic acid receptor gamma (RXR, matching the sequence from zebrafish *Danio rerio*) and found it did not change in abundance (ratio=0.85), similar to recent results in TH-treated *Xenopus* embryos [91]. Retinoic acid and RXR are known to be involved in retinal development [97-100], including retinoic acid's effect on rainbow trout UVS cone ontogeny in a manner similar to TH [39].

We also detected a peptide from a protein with similarity to a GI:30154764 homeobox protein that increased almost 25 fold during TH treatment. Various homeobox genes have been shown to be involved in retinal development [101-105]. Also of note was a peptide from an inhibitor of metalloproteinase that increased 9.5 fold in abundance, and a metalloproteinase peptide (both matched the sequence of cDNA clones from Atlantic salmon *Salmo salar*) that did not change in abundance (ratio=0.979). Matrix metalloproteinases are known to be regulated by TH [106] and are involved in tissue remodeling including retinal development and disease [107-109].

Perspective: Teleost retinas provide substantial advantages to understanding retinal development and function. The salmonid retina is a good example of this, with properties such as continued growth, regenerative capacity, and a highly ordered mosaic of photoreceptors (and other neurons) that facilitate a study of neuronal connectivity and interaction [110-112]. The salmonid retina has further interesting characteristics, including developmental plasticity of photoreceptors late in life history. This plasticity may be correlated with changes in the fish's environment, including migrations between deep-shallow or marine-freshwater habitats. Further, the large size of the salmonid eye compared to other popular teleost and rodent retinal models provides enough material for proteomic assessment of retinal development.

The approach we describe simultaneously identifies and quantifies the relative abundance of many proteins in two similar protein pools. By using commercially available facilities, one can quickly attain an overview of the retinal proteome and characterize changes in expression, even in rarely used animal models. Future work can help define criteria that establish guidelines for concluding that a given protein has changed in abundance. Like each high-throughput technique, repetition of results combined with confirmation through other approaches is required. The results of this study clearly demonstrate the potential of this technique to provide relevant and novel information in understanding retinal development and physiology.

REFERENCES

1. McKay GJ, Campbell L, Oliver M, Brockbank S, Simpson DA, Curry WJ. Preparation of planar retinal specimens: verification by histology, mRNA profiling, and proteome analysis. Mol Vis 2004; 10:240-7.
2. Swaroop A, Zack DJ. Transcriptome analysis of the retina. Genome Biol 2002; 3:REVIEWS1022.
3. Blackshaw S, Fraioli RE, Furukawa T, Cepko CL. Comprehensive analysis of photoreceptor gene expression and the identification of candidate retinal disease genes. Cell 2001; 107:579-89.
4. Gygi SP, Rochon Y, Franza BR, Aebersold R. Correlation between protein and mRNA abundance in yeast. Mol Cell Biol 1999; 19:1720-30.
5. Nishizawa Y, Komori N, Usukura J, Jackson KW, Tobin SL, Matsumoto H. Initiating ocular proteomics for cataloging bovine retinal proteins: microanalytical techniques permit the identification of proteins derived from a novel photoreceptor preparation. Exp Eye Res 1999; 69:195-212.
6. Matsumoto H, Komori N. Ocular proteomics: cataloging photoreceptor proteins by two-dimensional gel electrophoresis and mass spectrometry. Methods Enzymol 2000; 316:492-511.
7. Cavusoglu N, Thierse D, Mohand-Said S, Chalmel F, Poch O, Van-Dorsselaer A, Sahel JA, Leveillard T. Differential proteomic analysis of the mouse retina: the induction of crystallin proteins by retinal degeneration in the rd1 mouse. Mol Cell Proteomics 2003; 2:494-505.
8. Li D, Sun F, Wang K. Protein profile of aging and its retardation by caloric restriction in neural retina. Biochem Biophys Res Commun 2004; 318:253-8.
9. Yazulla S, Studholme KM. Neurochemical anatomy of the zebrafish retina as determined by immunocytochemistry. J Neurocytol 2001; 30:551-92.
10. Marc RE, Cameron D. A molecular phenotype atlas of the zebrafish retina. J Neurocytol 2001; 30:593-654.

11. Kunz YW, Wildenburg G, Goodrich L, Callaghan E. The fate of ultraviolet receptors in the retina of the Atlantic salmon (Salmo salar). Vision Res 1994; 34:1375-83.

12. Allison WT. Rainbow trout as a model of retinal photoreceptor death and regeneration [dissertation]. Victoria (Canada): University of Victoria; 2004.

13. Allison WT, Dann SG, Helvik JV, Bradley C, Moyer HD, Hawryshyn CW. Ontogeny of ultraviolet-sensitive cones in the retina of rainbow trout (Oncorhynchus mykiss). J Comp Neurol 2003; 461:294-306.

14. Allison WT, Dann SG, Veldhoen KM, Hawryshyn CW. Degeneration and regeneration of ultraviolet cone photoreceptors during development in rainbow trout. J Comp Neurol. In press 2006.

15. Hoar W. The physiology of smolting salmonids. In: Hoar WS, Randall DJ, editors. Fish physiology. New York: Academic Press; 1988. p. 275-343.

16. Coughlin DJ, Forry JA, McGlinchey SM, Mitchell J, Saporetti KA, Stauffer KA. Thyroxine induces transitions in red muscle kinetics and steady swimming kinematics in rainbow trout (Oncorhynchus mykiss). J Exp Zool 2001; 290:115-24.

17. Browman HI, Hawryshyn CW. Thyroxine induces a precocial loss of ultraviolet photosensitivity in rainbow trout (Oncorhynchus mykiss, Teleostei). Vision Res 1992; 32:2303-12.

18. Browman HI, Hawryshyn CW. The developmental trajectory of ultraviolet photosensitivity in rainbow trout is altered by thyroxine. Vision Res 1994; 34:1397-406.

19. Deutschlander ME, Greaves DK, Haimberger TJ, Hawryshyn CW. Functional mapping of ultraviolet photosensitivity during metamorphic transitions in a salmonid fish, Oncorhynchus mykiss. J Exp Biol 2001; 204:2401-13.

20. Hawryshyn CW, Martens G, Allison WT, Anholt BR. Regeneration of ultraviolet-sensitive cones in the retinal cone mosaic of thyroxin-challenged post-juvenile rainbow trout (Oncorhynchus mykiss). J Exp Biol 2003; 206:2665-73.

21. Beaudet L, Novales Flamarique I, Hawryshyn CW. Cone photoreceptor topography in the retina of sexually mature Pacific salmonid fishes. J Comp Neurol 1997; 383:49-59.

22. Beaudet L, Hawryshyn CW. Ecological aspects of vertebrate visual ontogeny. In: Archer SN, Djamgoz MBA, Loew ER, Partridge JC, Vallerga S, editors. Adaptive mechanisms in the ecology of vision. Dordrecht, The Netherlands: Kluwer; 1999. p 413-37.

23. Julian D, Ennis K, Korenbrot JI. Birth and fate of proliferative cells in the inner nuclear layer of the mature fish retina. J Comp Neurol 1998; 394:271-82.

24. Faillace MP, Julian D, Korenbrot JI. Mitotic activation of proliferative cells in the inner nuclear layer of the mature fish retina: regulatory signals and molecular markers. J Comp Neurol 2002; 451:127-41.

25. Allison WT, Hallows TE, Johnson T, Hawryshyn CW, Allen DM. Photic history modifies susceptibility to retinal damage in albino trout. Vis Neurosci. 2006; 23(1):25-34.

26. Veldhoen K, Allison WT, Veldhoen N, Anholt BR, Helbing CC, Hawryshyn CW. Spatio-temporal characterization of retinal opsin gene expression during thyroid hormone-induced and natural development of rainbow trout. Vis Neurosci 2006; 23:169-79.

27. Alexander G, Sweeting R, McKeown B. The shift in visual pigment dominance in the retinae of juvenile coho salmon (Oncorhynchus kisutch): an indicator of smolt status. J Exp Biol 1994; 195:185-97.

28. Beatty DD. Visual pigments and the labile scotopic visual system of fish. Vision Res 1984; 24:1563-73.

29. Bridges CDB. The rhodopsin-porphyropsin visual system. In: Dartnall HJ, editor. Handbook of Sensory Physiology. Vol. VII. Berlin: Springer-Verlag; 1972. p. 417-480.

30. Allison WT, Haimberger TJ, Hawryshyn CW, Temple SE. Visual pigment composition in zebrafish: Evidence for a rhodopsin-porphyropsin interchange system. Vis Neurosci 2004; 21:945-52. Erratum in: Vis Neurosci 2005; 22:249.

31. Beach DH, Jacobson M. Influences of thyroxine on cell proliferation in the retina of the clawed frog at different ages. J Comp Neurol 1979; 183:615-23.

32. Marsh-Armstrong N, Huang H, Remo BF, Liu TT, Brown DD. Asymmetric growth and development of the Xenopus laevis retina during metamorphosis is controlled by type III deiodinase. Neuron 1999; 24:871-8.

33. Plate EM, Adams BA, Allison WT, Martens G, Hawryshyn CW, Eales JG. The effects of thyroxine or a GnRH analogue on thyroid hormone deiodination in the olfactory epithelium and retina of rainbow trout, Oncorhynchus mykiss, and sockeye salmon, Oncorhynchus nerka. Gen Comp Endocrinol 2002; 127:59-65.

34. Orozco A, Linser P, Valverde C. Kinetic characterization of outer-ring deiodinase activity (ORD) in the liver, gill and retina of the killifish Fundulus heteroclitus. Comp Biochem Physiol B Biochem Mol Biol 2000; 126:283-90.

35. Ientile R, Macaione S, Russo P, Pugliese G, Di Giorgio RM. Phenolic and tyrosyl ring deiodination in thyroxine from rat retina during postnatal development. Eur J Biochem 1984; 142:15-9.

36. Ahlbert IB. Organization of the cone cells in the retinae of salmon (Salmo salar) and trout (Salmo trutta trutta) in relation to their feeding habits. Acta Zool 1976; 57:13-35.

37. Beaudet L, Browman HI, Hawryshyn CW. Optic nerve response and retinal structure in rainbow trout of different sizes. Vision Res 1993; 33:1739-46.

38. Bowmaker JK, Kunz YW. Ultraviolet receptors, tetrachromatic colour vision and retinal mosaics in the brown trout (Salmo trutta): age-dependent changes. Vision Res 1987; 27:2101-8.

39. Browman H, Hawryshyn C. Retinoic acid modulates retinal development in the juveniles of a teleost fish. J Exp Biol 1994; 193:191-207.

40. Browman HI, Gordon WC, Evans BI, O'Brien WJ. Correlation between histological and behavioral measures of visual acuity in a zooplanktivorous fish, the white crappie (Pomoxis annularis). Brain Behav Evol 1990; 35:85-97.

41. Kunz YW. Development of the eye of teleosts. In: Sensory biology of jawed fishes: new insights. Kapoor, BG and Hara, TJ, editor. Science Publishers, Inc., Enfield (NH); 2001. p. 1-18. ISBN: 1578080991.

42. Kunz YW. Tracts of putative ultraviolet receptors in the retina of the two-year-old brown trout (Salmo trutta) and the Atlantic salmon (Salmo salar). Experientia 1987; 43:1202-4.

43. Lyall AH. The growth of the trout retina. Quarterly Journal of Microscopical Science 1957; 98:101-110.

44. Lyall AH. Cone arrangements in teleost retinae. Quarterly Journal of Microscopical Science 1957; 98:189-201.

45. Flamarique I I, Hawryshyn C. Retinal development and visual sensitivity of young Pacific sockeye salmon (Oncorhynchus nerka). J Exp Biol 1996; 199:869-82.

46. Furst CM. Zur kenntnis der histogenese und des wachstums der retina. Lunds Universitets Årsskrift1904; 40:1-45.

47. Olson AJ, Picones A, Julian D, Korenbrot JI. A developmental time line in a retinal slice from rainbow trout. J Neurosci Methods 1999; 93:91-100.

48. Olson AJ, Picones A, Korenbrot JI. Developmental switch in excitability, Ca(2+) and K(+) currents of retinal ganglion cells and their dendritic structure. J Neurophysiol 2000; 84:2063-77.

49. Coughlin DJ, Hawryshyn CW. The contribution of ultraviolet and short-wavelength sensitive cone mechanisms to color vision in rainbow trout. Brain Behav Evol 1994; 43:219-32.

50. Coughlin DJ, Hawryshyn CW. Ultraviolet sensitivity in the torus semicircularis of juvenile rainbow trout (Oncorhynchus mykiss). Vision Res 1994; 34:1407-13.

51. Dann SG, Allison WT, Levin DB, Hawryshyn CW. Identification of a unique transcript down-regulated in the retina of rainbow trout (Oncorhynchus mykiss) at smoltification. Comp Biochem Physiol B Biochem Mol Biol 2003; 136:849-60.

52. Dann SG, Ted Allison W, Veldhoen K, Johnson T, Hawryshyn CW. Chromatin immunoprecipitation assay on the rainbow trout opsin proximal promoters illustrates binding of NF-kappaB and c-jun to the SWS1 promoter in the retina. Exp Eye Res 2004; 78:1015-24.

53. Veldhoen K, Beaudet L, Runions J, Sharma S, Hawryshyn CW. Antibody labeling of the blue-sensitive cones in the retinae of teleost fishes. Can J Zool 1999; 77:1733-9.

54. Ekstrom P, Anzelius M. GABA and GABA-transporter (GAT-1) immunoreactivities in the retina of the salmon (Salmo salar L.). Brain Res 1998; 812:179-85.

55. Koppang EO, Bjerkas E, Bjerkas I, Sveier H, Hordvik I. Vaccination induces major histocompatibility complex class II expression in the Atlantic salmon eye. Scand J Immunol 2003; 58:9-14.

56. Vecino E, Garcia-Brinon J, Velasco A, Caminos E, Lara J. Calbindin D-28K distribution in the retina of the developing trout (Salmo fario L.). Neurosci Lett 1993; 152:91-5.

57. Vecino E. Spatiotemporal development of the fish retina: distribution of calbindin D-28K. Semin Cell Dev Biol 1998; 9:271-7.

58. Candal EM, Caruncho HJ, Sueiro C, Anadon R, Rodriguez-Moldes I. Reelin expression in the retina and optic tectum of developing common brown trout. Brain Res Dev Brain Res 2005; 154:187-97.

59. Candal E, Anadon R, DeGrip WJ, Rodriguez-Moldes I. Patterns of cell proliferation and cell death in the developing retina and optic tectum of the brown trout. Brain Res Dev Brain Res 2005; 154:101-19.

60. Drescher DG, Ramakrishnan NA, Drescher MJ, Chun W, Wang X, Myers SF, Green GE, Sadrazodi K, Karadaghy AA, Poopat N, Karpenko AN, Khan KM, Hatfield JS. Cloning and characterization of alpha9 subunits of the nicotinic acetylcholine receptor expressed by saccular hair cells of the rainbow trout (Oncorhynchus mykiss). Neuroscience 2004; 127:737-52.

61. Weruaga E, Velasco A, Brinon JG, Arevalo R, Aijon J, Alonso JR. Distribution of the calcium-binding proteins parvalbumin, calbindin D-28k and calretinin in the retina of two teleosts. J Chem Neuroanat 2000; 19:1-15.

62. Malz CR, Kindermann U. Establishment of the FMRFamide-immunoreactive olfacto-retinalis pathway during ontogeny of the rainbow trout (Oncorhynchus mykiss). J Hirnforsch 1999; 39:349-53.

63. Ostholm T, Holmqvist BI, Alm P, Ekstrom P. Nitric oxide synthase in the CNS of the Atlantic salmon. Neurosci Lett 1994; 168:233-7.

64. Wagner HJ, Behrens UD. Microanatomy of the dopaminergic system in the rainbow trout retina. Vision Res 1993; 33:1345-58.

65. Holmqvist BI, Ostholm T, Ekstrom P. DiI tracing in combination with immunocytochemistry for analysis of connectivities and chemoarchitectonics of specific neural systems in a teleost, the Atlantic salmon. J Neurosci Methods 1992; 42:45-63.

66. Rime H, Guitton N, Pineau C, Bonnet E, Bobe J, Jalabert B. Post-ovulatory ageing and egg quality: a proteomic analysis of rainbow trout coelomic fluid. Reprod Biol Endocrinol 2004; 2:26.

67. Martin SA, Vilhelmsson O, Medale F, Watt P, Kaushik S, Houlihan DF. Proteomic sensitivity to dietary manipulations in rainbow trout. Biochim Biophys Acta 2003; 1651:17-29.

68. Kanaya S, Ujiie Y, Hasegawa K, Sato T, Imada H, Kinouchi M, Kudo Y, Ogata T, Ohya H, Kamada H, Itamoto K, Katsura K. Proteome analysis of Oncorhynchus species during embryogenesis. Electrophoresis 2000; 21:1907-13.

69. Gygi SP, Rist B, Gerber SA, Turecek F, Gelb MH, Aebersold R. Quantitative analysis of complex protein mixtures using isotope-coded affinity tags. Nat Biotechnol 1999; 17:994-9.

70. Li K, Hornshaw MP, van Minnen J, Smalla KH, Gundelfinger ED, Smit AB. Organelle proteomics of rat synaptic proteins: correlation-profiling by isotope-coded affinity tagging in conjunction with liquid chromatography-tandem mass spectrometry to reveal post-synaptic density specific proteins. J Proteome Res 2005; 4:725-33.

71. Liu L, Chen S, Yang Q, Kang K, McCormick TS, Cooper KD. Cleavable 13C-isotope-coded affinity tag (clCAT) with in-line 2D-LC-ESI mass spectrometry for proteomic analysis of membrane proteins in keratinocytes following UVB exposure. Journal of Investigative Dermatology 2005; 124:A137.

72. Pisitkun T, Wang GH, Wu W, Knepper MA. Proteomic analysis of long-term vasopressin action in the inner medullary collecting duct (IMCD) using isotope-coded affinity tag technique. FASEB J 2005; 19:A1607.

73. Sinclair G, Yip K, Clarke LA. Serum prefactionation for isotope-coded affinity tag (ICAT) proteomics and biomarker identification in a murine model of MPS. Mol Genet Metab 2005; 84:236-7.

74. Booy AT, Haddow JD, Ohlund LB, Hardie DB, Olafson RW. Application of isotope coded affinity tag (ICAT) analysis for the identification of differentially expressed proteins following infection of atlantic salmon (Salmo salar) with infectious hematopoietic necrosis virus (IHNV) or Renibacterium salmoninarum (BKD). J Proteome Res 2005; 4:325-34.

75. Yu LR, Conrads TP, Uo T, Issaq HJ, Morrison RS, Veenstra TD. Evaluation of the acid-cleavable isotope-coded affinity tag reagents: application to camptothecin-treated cortical neurons. J Proteome Res 2004; 3:469-77.

76. Meehan KL, Sadar MD. Quantitative profiling of LNCaP prostate cancer cells using isotope-coded affinity tags and mass spectrometry. Proteomics 2004; 4:1116-34.

77. Li KW, Hornshaw MP, Van Der Schors RC, Watson R, Tate S, Casetta B, Jimenez CR, Gouwenberg Y, Gundelfinger ED, Smalla KH, Smit AB. Proteomics analysis of rat brain postsynaptic density. Implications of the diverse protein functional groups for the integration of synaptic physiology. J Biol Chem 2004; 279:987-1002.

78. Rise ML, von Schalburg KR, Brown GD, Mawer MA, Devlin RH, Kuipers N, Busby M, Beetz-Sargent M, Alberto R, Gibbs AR, Hunt P, Shukin R, Zeznik JA, Nelson C, Jones SR, Smailus DE, Jones SJ, Schein JE, Marra MA, Butterfield YS, Stott JM, Ng SH, Davidson WS, Koop BF. Development and application of a salmonid EST database and cDNA microarray: data mining

and interspecific hybridization characteristics. Genome Res 2004; 14:478-90.

79. Dann SG, Allison WT, Levin DB, Taylor JS, Hawryshyn CW. Salmonid opsin sequences undergo positive selection and indicate an alternate evolutionary relationship in oncorhynchus. J Mol Evol 2004; 58:400-12.

80. Lema SC, Nevitt GA. Evidence that thyroid hormone induces olfactory cellular proliferation in salmon during a sensitive period for imprinting. J Exp Biol 2004; 207:3317-27.

81. Monte M, Benetti R, Buscemi G, Sandy P, Del Sal G, Schneider C. The cell cycle-regulated protein human GTSE-1 controls DNA damage-induced apoptosis by affecting p53 function. J Biol Chem 2003; 278:30356-64.

82. Collavin L, Monte M, Verardo R, Pfleger C, Schneider C. Cell-cycle regulation of the p53-inducible gene B99. FEBS Lett 2000; 481:57-62.

83. Galli-Resta L, Novelli E, Viegi A. Dynamic microtubule-dependent interactions position homotypic neurones in regular monolayered arrays during retinal development. Development 2002; 129:3803-14.

84. Goldman D, Ding J. Different regulatory elements are necessary for alpha1 tubulin induction during CNS development and regeneration. Neuroreport 2000; 11:3859-63.

85. Schenker M, Riederer BM, Kuntzer T, Barakat-Walter I. Thyroid hormones stimulate expression and modification of cytoskeletal protein during rat sciatic nerve regeneration. Brain Res 2002; 957:259-70.

86. van Doorn KL, Sivak JG, Vijayan MM. Optical quality changes of the ocular lens during induced parr-to-smolt metamorphosis in Rainbow Trout (Oncorhynchus mykiss). Ocular lens optical quality during induced salmonid metamorphosis. J Comp Physiol A Neuroethol Sens Neural Behav Physiol 2005; 191:649-57.

87. McCormick SD. Endocrine control of osmoregulation in teleost fish. American Zoologist 2001; 41:781-94.

88. Zhang H, Futami K, Yamada Y, Horie N, Okamura A, Utoh T, Mikawa N, Tanaka S, Okamoto N, Oka HP. Isolation of freshwater and deep-sea type opsin genes from the common Japanese conger. Journal of Fish Biology 2002; 61:313-24.

89. Archer S, Hope A, Partridge JC. The molecular basis for the green-blue sensitivity shift in the rod visual pigments of the European eel. Proc Biol Sci 1995; 262:289-95.

90. Minamoto T, Shimizu I. Molecular cloning and characterization of rhodopsin in a teleost (Plecoglossus altivelis, Osmeridae). Comp Biochem Physiol B Biochem Mol Biol 2003; 134:559-70.

91. Cossette SM, Drysdale TA. Early expression of thyroid hormone receptor beta and retinoid X receptor gamma in the Xenopus embryo. Differentiation 2004; 72:239-49.

92. Philp AR, Bellingham J, Garcia-Fernandez J, Foster RG. A novel rod-like opsin isolated from the extra-retinal photoreceptors of teleost fish. FEBS Lett 2000; 468:181-8. Erratum in: FEBS Lett 2000; 473:125-6.

93. Appel B, Eisen JS. Regulation of neuronal specification in the zebrafish spinal cord by Delta function. Development 1998; 125:371-80.

94. Perron M, Harris WA. Determination of vertebrate retinal progenitor cell fate by the Notch pathway and basic helix-loop-helix transcription factors. Cell Mol Life Sci 2000; 57:215-23.

95. Neumann CJ. Pattern formation in the zebrafish retina. Semin Cell Dev Biol 2001; 12:485-90.

96. Bernardos RL, Lentz SI, Wolfe MS, Raymond PA. Notch-Delta signaling is required for spatial patterning and Muller glia differentiation in the zebrafish retina. Dev Biol 2005; 278:381-95.

97. Hoover F, Seleiro EA, Kielland A, Brickell PM, Glover JC. Retinoid X receptor gamma gene transcripts are expressed by a subset of early generated retinal cells and eventually restricted to photoreceptors. J Comp Neurol 1998; 391:204-13.

98. Marsh-Armstrong N, McCaffery P, Gilbert W, Dowling JE, Drager UC. Retinoic acid is necessary for development of the ventral retina in zebrafish. Proc Natl Acad Sci U S A 1994; 91:7286-90.

99. Kelley MW, Williams RC, Turner JK, Creech-Kraft JM, Reh TA. Retinoic acid promotes rod photoreceptor differentiation in rat retina in vivo. Neuroreport 1999; 10:2389-94.

100. Chen DM, Dong G, Stark WS. Ultraviolet light damage and reversal by retinoic acid in juvenile goldfish retina. In: Hollyfield JG, Anderson RE, LaVail MM, editors. Retinal Degenerative Diseases and Experimental Therapy. Proceedings of the 8th International Symposium on Retinal Degenerations; 1998 Nov 23-27; Schluchsee, Germany. New York: Kluwer Academic/Plenum; 1999. p. 325-36.

101. Chuang JC, Raymond PA. Zebrafish genes rx1 and rx2 help define the region of forebrain that gives rise to retina. Dev Biol 2001; 231:13-30.

102. Shen YC, Raymond PA. Zebrafish cone-rod (crx) homeobox gene promotes retinogenesis. Dev Biol 2004; 269:237-51.

103. Lupo G, Andreazzoli M, Gestri G, Liu Y, He RQ, Barsacchi G. Homeobox genes in the genetic control of eye development. Int J Dev Biol 2000; 44:627-36.

104. Mathers PH, Jamrich M. Regulation of eye formation by the Rx and pax6 homeobox genes. Cell Mol Life Sci 2000; 57:186-94.

105. Levine EM, Green ES. Cell-intrinsic regulators of proliferation in vertebrate retinal progenitors. Semin Cell Dev Biol 2004; 15:63-74.

106. Jung JC, West-Mays JA, Stramer BM, Byrne MH, Scott S, Mody MK, Sadow PM, Krane SM, Fini ME. Activity and expression of Xenopus laevis matrix metalloproteinases: identification of a novel role for the hormone prolactin in regulating collagenolysis in both amphibians and mammals. J Cell Physiol 2004; 201:155-64. Erratum in: J Cell Physiol 2004; 201:165.

107. Chintala SK, Zhang X, Austin JS, Fini ME. Deficiency in matrix metalloproteinase gelatinase B (MMP-9) protects against retinal ganglion cell death after optic nerve ligation. J Biol Chem 2002; 277:47461-8.

108. Zhang X, Sakamoto T, Hata Y, Kubota T, Hisatomi T, Murata T, Ishibashi T, Inomata H. Expression of matrix metalloproteinases and their inhibitors in experimental retinal ischemia-reperfusion injury in rats. Exp Eye Res 2002; 74:577-84.

109. Sivak JM, Fini ME. MMPs in the eye: emerging roles for matrix metalloproteinases in ocular physiology. Prog Retin Eye Res 2002; 21:1-14.

110. Stenkamp DL, Hisatomi O, Barthel LK, Tokunaga F, Raymond PA. Temporal expression of rod and cone opsins in embryonic goldfish retina predicts the spatial organization of the cone mosaic. Invest Ophthalmol Vis Sci 1996; 37:363-76.

111. Easter SS, Hitchcock PF. Stem cells and regeneration in the retina: What fish have taught us about neurogenesis. Neuroscientist 2000; 6:454-64.

112. Raymond PA, Barthel LK. A moving wave patterns the cone photoreceptor mosaic array in the zebrafish retina. Int J Dev Biol 2004; 48:935-45.

Appendix 1. The appendix is available in the online version of this article at http://www.molvis.org/molvis/v12/a74/.